processes

MDPI

Article

The Effects of the Acid Treatment of ZrB_2 Particles on Their Purity and Aqueous Dispersibility

Jinuk Choi [1] and Gye Seok An [2,*]

[1] Division of Materials Science and Engineering, Hanyang University, 222 Wangsimni-ro, Seongdong-gu, Seoul 04763, Korea; wls2117@hanyang.ac.kr
[2] Department of Advanced Materials Engineering, Kyonggi University, 154-42 Gwanggyosan-ro, Yeongtong-gu, Suwon 16227, Korea
* Correspondence: gsmaroan@kyonggi.ac.kr

Abstract: Oxide impurities such as boria (B_2O_3) and zirconia (ZrO_2) on the surfaces of zirconium diboride (ZrB_2) particles are known to limit their sinterability. Among the impurities, B_2O_3 on the surface of ZrB_2 particles could be easily removed by methanol or hydrofluoric acid. However, the remaining ZrO_2 still gave negative influences on the sinterability. In this study, ZrB_2 particles were treated with various acids to remove oxide impurities on their surfaces. The acid treatments were found to vary in efficacy, according to acid type, and affect the crystallinity and morphology of ZrB_2 particles to varying degrees, in some cases forming additional impurities. In particular, the change in the oxygen content of the ZrB_2 particles induced by acid treatment was found to depend on the type of acid. The results of the acid treatments were compared which revealed that HNO_3 treatment optimizes the purity of ZrB_2 particles. In addition, the effects of acid treatment on the surface properties of ZrB_2 particles were considered. In particular, the correlation between the surface properties of the acid-treated ZrB_2 particles and their dispersibility in aqueous solution was investigated.

Keywords: zirconium diboride; acid-treatment; zeta potential; oxygen contents; dispersibility

check for updates

Citation: Choi, J.; An, G.S. The Effects of the Acid Treatment of ZrB_2 Particles on Their Purity and Aqueous Dispersibility. *Processes* **2022**, *10*, 18. https://doi.org/10.3390/pr10010018

Academic Editor: Mingxia Gao

Received: 9 December 2021
Accepted: 21 December 2021
Published: 23 December 2021

Publisher's Note: MDPI stays neutral with regard to jurisdictional claims in published maps and institutional affiliations.

Copyright: © 2021 by the authors. Licensee MDPI, Basel, Switzerland. This article is an open access article distributed under the terms and conditions of the Creative Commons Attribution (CC BY) license (https://creativecommons.org/licenses/by/4.0/).

1. Introduction

A critical factor affecting the development of aerospace technologies such as hypersonic flight vehicles is the requirement for materials with high-temperature tolerance, excellent mechanical strength, and oxidation resistance [1–3]. A specific class of materials developed for use under extreme environmental conditions is ultra-high-temperature ceramics (UHTCs) and research interest in this class of materials is increasing [1–4].

Among UHTCs, zirconium diboride (ZrB_2) is especially suitable for application in extreme environments owing to properties such as a high melting point (3246 °C); high-temperature stability and strength; high electrical and thermal conductivities; excellent corrosion resistance and hardness; a high elastic modulus; and a chemically stable crystal structure [5–11]. These physicochemical properties result from its strong covalent bonds and low self-diffusion coefficient [5–7,12].

However, these properties of ZrB_2 that inform its classification as a UHTC also contribute to its limited sinterability [13–15]. Moreover, an incidental reduction is caused by the unavoidable oxide impurities in non-oxide inorganic materials [14–16]. Oxide impurities such as boron trioxide (B_2O_3) and zirconium dioxide (ZrO_2) were formed easily on ZrB_2 particles during milling processes or storage due to moisture in the atmosphere [17–20]. Amorphous B_2O_3 impurities enable rapid diffusion to accelerate coarsening. During grain coarsening, the surface area of the particles decreases as the driving force for densification is consumed, thus having a negative influence on the sinterability of ZrB_2 [17,18,20–22]. A previous study showed that most of the B_2O_3 content of ZrB_2 powder can be removed by washing the powder with methanol [14,20]. In contrast, ZrO_2, another significant oxide impurity, is chemically stable, regardless of its crystalline phase, and is difficult to remove.

This study investigated the efficacy of acid treatment in enhancing the purity of commercial ZrB_2 powder, i.e., removing Zr–O impurities which are one of the main factors limiting the sinterability of ZrB_2. The effects of acid treatment (using various acids) on the surface properties, microstructure, and aqueous dispersibility of ZrB_2 particles were studied.

2. Materials and Methods

2.1. Pretreatment of ZrB_2 Particles with Methanol

Commercial ZrB_2 powder (Japan New Metals Co., Osaka, Japan), with a mean particle size of 2.61 μm, was used as a starting material. To eliminate oxides like B_2O_3, the ZrB_2 powder was subjected to repeated washing processes, and each time it was ultrasonicated during centrifugation in 40 mL methanol (99.9%, Daejung Chemicals and Metals Co., Siheung, Korea) for 10 min [14]. The washed particles were dried in a vacuum drying oven under a pressure of −0.1 MPa at 40 °C for 12 h.

2.2. Treatment of ZrB_2 Particles with Various Acids

The surfaces of methanol-washed, commercial ZrB_2 particles were modified through treatment with various acids, namely hydrochloric acid (HCl, 36.46%, Daejung Chemicals and Metals Co., Siheung, Korea), nitric acid (HNO_3, 61%, Junsei Chemical Co., Tokyo, Japan), sulfuric acid (H_2SO_4, >98%, Daejung Chemicals and Metals Co., Korea), and hydrofluoric acid (HF, 50.5%, Duksan Pure Chemicals, Ansan, Korea). The acquired acids were diluted with deionized (DI) water to a concentration of 1 mol% to enable the comparison of their effects on ZrB_2 particles. Methanol-washed ZrB_2 powder (5 g) and diluted acid (250 mL) were mixed at 300 rpm for 1 h at 80 °C in a 500 mL three-necked round-bottom flask and then cooled to room temperature. Each modified ZrB_2 powder was subjected to repeated methanol washing processes to remove residual acid; each time it was ultrasonicated during centrifugation. The washed particles were dried in a vacuum drying oven under a pressure of −0.1 MPa at 40 °C for 12 h.

2.3. Characterization

The crystallinity of the ZrB_2 particles was analyzed by X-ray diffraction (XRD; Ultima IV, Rigaku, Japan) using CuKα radiation (wavelength (λ) = 1.54178Å). The microstructures of the particles were analyzed by field emission scanning electron microscopy (FE-SEM; JSM-6330F, JEOL, Tokyo, Japan). To determine the oxide impurities, the oxygen content of the particles was investigated using a carrier gas hot extraction method (TC-600, LECO Co., St. Joseph, MI, USA). The surface properties of the particles were determined by Fourier transform infrared spectroscopy (FT-IR; IRAffinity-1 S, Shimadzu, Kyoto, Japan). The zeta potential and the particle size distribution (PSD) was determined using the dynamic light scattering (Zetasizer Nano ZSP, Malvern, PA, USA) method.

3. Results and Discussion

ZrO_2, an oxide impurity that acts as a sintering inhibitor of ZrB_2, exists on the surface rather than within ZrB_2 particles, considering that it is formed mainly as a result of water in the atmosphere [17]. Therefore, it was accepted that the acids in this study react with ZrO_2 on the surface of ZrB_2 particles according to the following chemical reactions [19,23]:

$$ZrO_2 + 6HCl \rightarrow [ZrCl_6]^{2-} + 2H_3O^+ \quad (1)$$

$$ZrO_2 + 6HNO_3 \rightarrow [Zr(NO_3)_6]^{2-} + 2H_3O^+ \quad (2)$$

$$ZrO_2 + 2H_2SO_4 \rightarrow [Zr(SO_4)_2]^{2-} + 2H_3O^+ \quad (3)$$

$$ZrO_2 + 6HF \rightarrow [ZrF_6]^{2-} + 2H_3O^+ \quad (4)$$

Figure 1 shows the XRD patterns of as-received ZrB_2 particles and acid-treated ZrB_2 particles. In the XRD patterns of the as-received ZrB_2 particles, diffraction peaks are

observed at 25.2°, 32.5°, 41.5°, and 51.5°; these peaks correspond to the (011), (100), (101), and (002) planes, respectively, of hexagonal ZrB_2 (JCPDS no. 89-3930). The XRD patterns of the HCl- and HNO_3-treated ZrB_2 particles do not differ significantly from that of the as-received ZrB_2 particles; suggesting that HCl and HNO_3 treatments do not significantly affect the crystallinity and structure of ZrB_2 particles. On the other hand, the XRD patterns of the H_2SO_4- and HF-treated ZrB_2 particles differ significantly from that of the as-received ZrB_2 particles; the peaks observed in the XRD of the as-received ZrB_2 particles are barely discernable in the XRD of the H_2SO_4- and HF-treated ZrB_2 particles and a number of new low-intensity peaks are observed. The XRD peaks observed at 30.2° and 50.2° correspond to the (101), (110), and (112) planes, respectively, of tetragonal ZrO_2 (JCPDS no. 81-1544), while the peaks at 28.1°, 31.4°, 34.9°, and 50.1° correspond to the (-111), (111), (020), and (220) planes, respectively, of monoclinic ZrO_2 (JCPDS no. 81-1314). The XRD peaks at 22.0°, 23.4°, 34.9°, and 37.7° correspond to the (003), (012), (104), and (021) planes, respectively, of B_4C (JCPDS no. 86-1129). In particular, the XRD of H_2SO_4-treated ZrB_2 particles shows peaks at 30.1°, 35.4°, and 50.4°, corresponding to the (101), (110), and (112) planes, respectively, of sulfated zirconia (SZ) (JCPDS no. 80-2155); as well as peaks at 28.1°, 32.5°, 41.5°, and 50.1°, corresponding to the (100), (101), (102), and (110) planes of ZrS_2 (JCPDS no. 11-0679) [24,25]. Oxidation produced both tetragonal and monoclinic ZrO_2 while H_2SO_4 and HF dissolved the ZrB_2 particles. SZ was formed because SO_4^{2-} from H_2SO_4 attached to the ionized surface of ZrO_2 formed by oxidation. The unexpected peaks associated with B_4C is likely owed to the presence of small quantities of B_4C within the commercial ZrB_2 particles that are released by the acid treatment, i.e., the dissolution of the ZrB_2 particles.

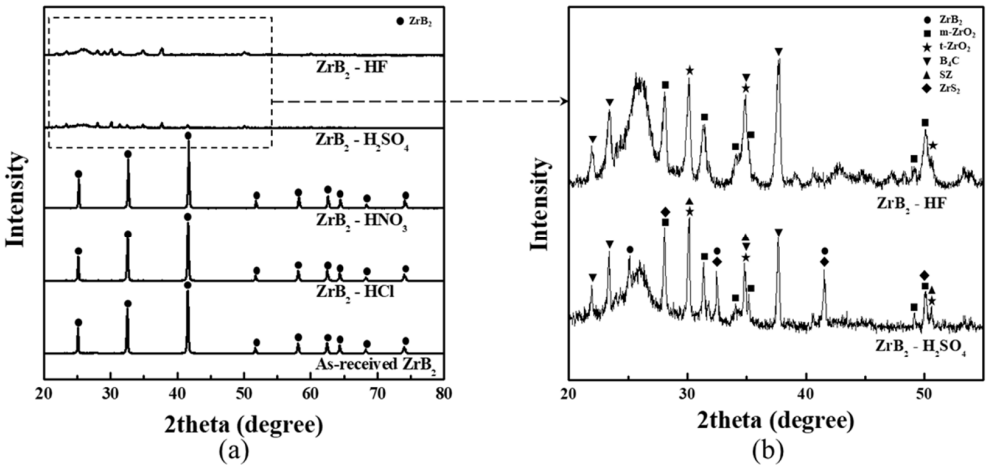

Figure 1. X-ray diffraction (XRD) patterns of different samples. (**a**) XRD patterns of as-received ZrB_2 particles and acid-treated ZrB_2 particles and (**b**) the specific part of XRD patterns of HF- and H_2SO_4-treated ZrB_2.

Figure 2 shows the microstructures of as-received ZrB_2 particles, methanol-washed ZrB_2 particles, and HCl-, HNO_3-, H_2SO_4-, and HF-treated ZrB_2 particles. The as-received ZrB_2 particles have roundish shapes, however, the roundish shapes of the HCl- and HNO_3-treated ZrB_2 particles are more distinct. The morphologies of the HCl- and HNO_3-treated ZrB_2 particles are similar, exhibiting fairly smooth surfaces. Unlike the HCl- and HNO_3-treated ZrB_2 particles, the H_2SO_4-treated ZrB_2 particles (which also produced distinct XRD patterns), appear aggregated and merged. In particular, the morphology of HF-treated ZrB_2 particles is unique, as shown in Figure 2f, exhibiting a rhapis shape. During acid treatment, H_2SO_4 and HF dissolve ZrB_2 particles and transform them from ZrB_2 to oxide phases, monoclinic ZrO_2 and tetragonal ZrO_2, which contain significant amounts of oxygen, and SZ in the case of H_2SO_4; as revealed by the XRD results (Figure 1). The various shapes of the acid-treated ZrB_2 particles suggest that their properties are dissimilar. To elucidate the differences in the properties of the various ZrB_2 particles, they were quantitatively analyzed.

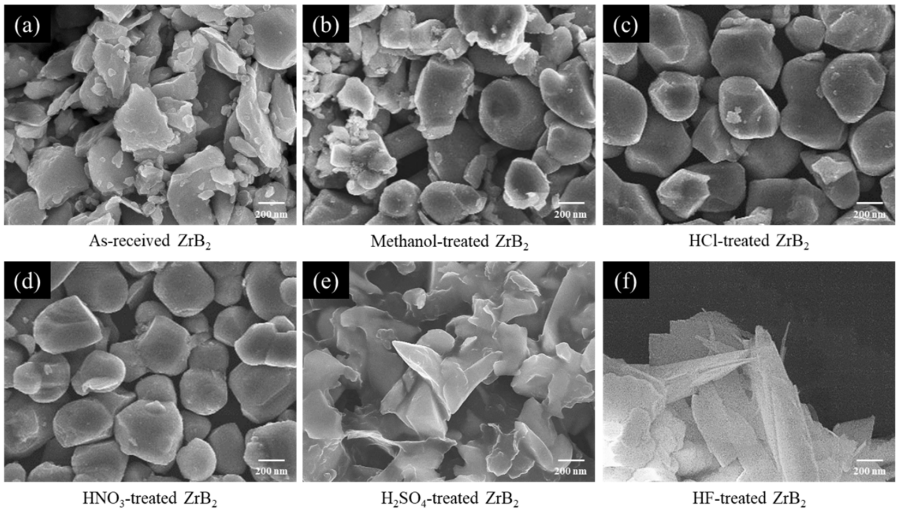

Figure 2. Scanning electron microscopy (SEM) images of (**a**) as-received ZrB_2, (**b**) methanol-treated ZrB_2, (**c**) HCl-, (**d**) HNO_3-, (**e**) H_2SO_4-, and (**f**) HF-treated ZrB_2 particles.

Figure 3 shows the oxygen contents of ZrB_2 particles subjected to 0 to 4 washing processes in methanol. The major oxide impurities on the surfaces of ZrB_2 particles are ZrO_2 and B_2O_3 [26]. A previous study revealed that B_2O_3 on the surfaces of ZrB_2 particles can be efficiently dissolved in methanol [6]. Accordingly, commercial ZrB_2 particles were subject to repeated washing processes, each time the particles were ultrasonicated during centrifugation in 40 mL methanol for 10 min. The initial oxygen content of the commercial ZrB_2 particles was 3.52 ± 0.19 wt%. After three and four washing processes in methanol, the oxygen contents of the ZrB_2 particles are 1.28 ± 0.13 wt% and 1.23 ± 0.09 wt%, respectively. It was found that the washing processes in methanol are unable to reduce the oxygen content of the commercial ZrB_2 particles to less than approximately 1.2 wt%. The oxygen contents of ZrB_2 particles subjected to three and four washing processes are not significantly different; however, the standard deviation in the oxygen content of ZrB_2 particles subjected to four washing processes is noticeably lower than the standard deviation in the oxygen content of ZrB_2 particles subject to three washing processes. Despite the efficacy of the washing process, the oxygen content of the ZrB_2 particles still exceeds 1 wt% owing to the presence of ZrO_2.

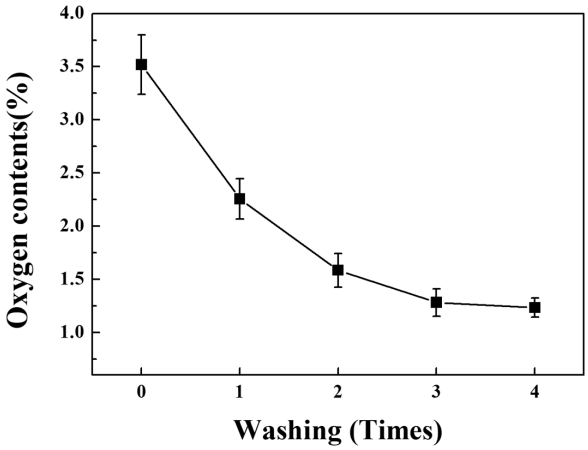

Figure 3. Oxygen contents of ZrB_2 particles via methanol treatment.

It was found that treating the methanol-washed ZrB_2 particles with HCl, reduced their oxygen content from 1.23 ± 0.09 wt% to 0.56 ± 0.06 wt% as shown in Table 1. Similarly, the oxygen content of HNO_3-treated ZrB_2 particles was relatively low at 0.54 ± 0.04 wt%.

The oxygen content and the standard deviation in the oxygen content of HNO_3-treated ZrB_2 particles was lower than those of HCl-treated ZrB_2 particles. The removal of oxide impurities on the surface of the ZrB_2 particles could be deduced based on the reduction in oxygen content. The treatment of methanol-washed ZrB_2 particles with H_2SO_4 and HF increased their oxygen content to 15.04 ± 1.46 wt% and 12.66 ± 1.80 wt%, respectively. The oxygen contents of the HCl- and HNO_3-treated ZrB_2 particles were lower than those of the H_2SO_4- and HF-treated ZrB_2 particles owing to the high reactivity of H_2SO_4 and HF towards ZrB_2. The increase in oxygen contents of H_2SO_4- and HF-treated ZrB_2 particles was consistent with the change in the crystallinity of ZrB_2 particles induced by H_2SO_4 and HF treatments, as shown in the XRD results (Figure 1). These results revealed that H_2SO_4 and HF treatments were ineffective at reducing the oxygen content of ZrB_2 particles. Consequently, only HCl and HNO_3 treatments were investigated further.

Table 1. The oxygen contents of as-prepared of ZrB_2 and acid-treated ZrB_2.

Materials	Oxygen Contents (%)	Standard Deviation (%)
Methanol-treated ZrB_2	1.23	0.09
HCl-treated ZrB_2	0.56	0.06
HNO_3-treated ZrB_2	0.54	0.04
H_2SO_4-treated ZrB_2	15.04	1.46
HF-treated ZrB_2	12.66	1.80

Figure 4 shows the zeta potentials of as-received ZrB_2 particles and HCl- and HNO_3-treated ZrB_2 particles. The zeta potential of the as-received ZrB_2 particles is −11.3 ± 0.98 mV. In contrast, the zeta potentials of the HCl- are HNO_3-treated ZrB_2 particles are −33.4 ± 0.47 mV and −40.2 ± 0.46 mV, respectively. The zeta potentials and standard deviation in the zeta potentials of the acid-treated ZrB_2 particles are lower than those of the as-received ZrB_2 particles; moreover, the zeta potential and standard deviation in the zeta potential of the HNO_3-treated ZrB_2 particles are lower than those of the HCl-treated ZrB_2 particles. Evidently, HCl and HNO_3 treatments increase the absolute zeta potential of ZrB_2 particles.

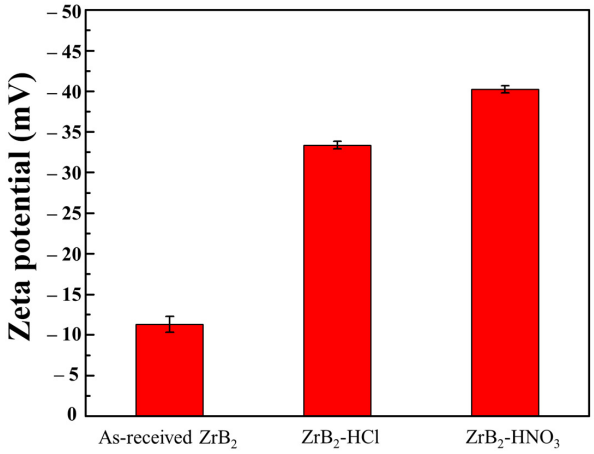

Figure 4. Zeta potentials of as-received ZrB_2, HCl-treated ZrB_2, and HNO_3-treated ZrB_2 particles.

Figure 5 shows the FT-IR spectra of as-received ZrB_2 particles and HCl- and HNO_3-treated ZrB_2 particles. The spectrum of the as-received ZrB_2 particles shows peaks at 3221 cm^{-1} and 1477 cm^{-1} corresponding to O–H stretching vibrations and C–H bending vibrations, respectively. The spectra of the HCl- and HNO_3-treated ZrB_2 particles are similar to that of the as-received ZrB_2 particles; however, the intensities of the O–H peaks in the spectra of the acid-treated ZrB_2 particles are higher than that of the O–H peak in the spectrum of the as-received ZrB_2 particles. Additionally, in the spectrum of the HNO_3-treated ZrB_2 particles, a low-intensity peak is observed at 1525 cm^{-1} corresponding to

N–O stretching vibrations. The hydroxyl groups on the surfaces of the acid-treated ZrB_2 particles enhance the electrostatic repulsion of the particles, accounting for the relatively low zeta potentials of the acid-treated ZrB_2 particles (Figure 4). The observed N–O peak in the spectrum of the HNO_3-treated ZrB_2 particles is likely caused by the reaction of ZrB_2 with the nitrogen in HNO_3.

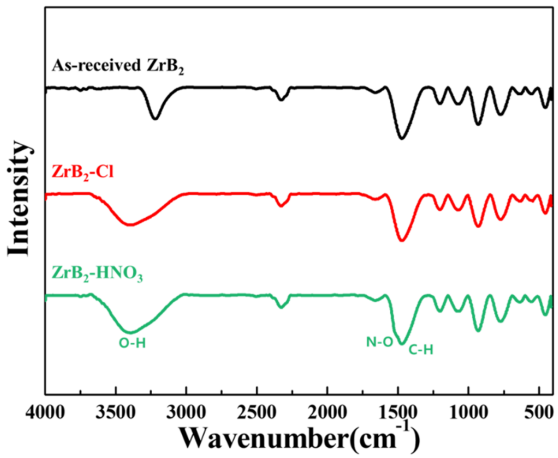

Figure 5. Fourier transform infrared (FT-IR) spectra of as-received ZrB_2, HCl-treated ZrB_2, and HNO_3-treated ZrB_2 particles.

Figure 6 shows the PSD of as-received ZrB_2 particles and HCl- and HNO_3-treated ZrB_2 particles in DI water. The as-received ZrB_2 particles show a wide and bimodal PSD with peaks at 697 nm and 1977 nm. In contrast, the HCl- and HNO_3-treated ZrB_2 particles show monomodal PSDs with peaks at 691 nm and 583 nm, respectively. The mean size of the HNO_3-treated ZrB_2 particles (631 nm) is less than that of the HCl-treated ZrB_2 particles (778 nm). The differences in the PSD curves are related to the electrostatic repulsion of the particles. Particles with higher absolute zeta potential are more dispersed (Figure 4). The bimodal PSD of the as-received ZrB_2 particles is due to the aggregation of the particles resulting from insufficient electrostatic repulsion. The HCl and HNO_3 treatment of ZrB_2 particles enhance their dispersibility; accounting for the monomodal PSDs of the HCl- and HNO_3-treated ZrB_2 particles. Evidently, acid treatment enhances the dispersion of ZrB_2 particles; however, HNO_3 treatment is more effective than HCl treatment in enhancing the dispersion of ZrB_2 particles as it induces a higher absolute zeta potential in ZrB_2 particles than HCl treatment.

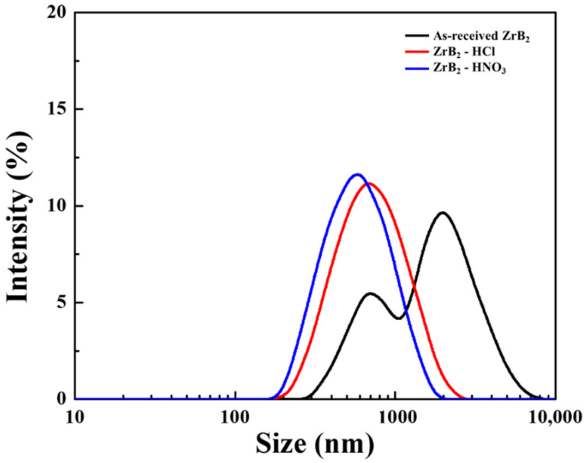

Figure 6. Particle size distribution (PSD) of as-received ZrB_2, HCl-treated ZrB_2, and HNO_3-treated ZrB_2 particles.

4. Conclusions

Oxide impurities are formed on ZrB_2 particles during milling processes and storage because of moisture in the atmosphere; this phenomenon is exacerbated by the large surface area and high surface energy of ZrB_2 particles. Oxide impurities, such as ZrO_2 and B_2O_3, limit the sinterability of ZrB_2 particles. In this study, washing processes with methanol and acid treatments were performed to remove the oxygen impurities on commercial ZrB_2 particles. The oxygen content of ZrB_2 particles is reduced by washing the particles in methanol, owing to the removal of B_2O_3; however, oxygen impurities such as ZrO_2 remain. To remove ZrO_2 impurities, the methanol-washed ZrB_2 particles were treated with various acids. HCl and HNO_3 treatments were found to preserve the crystallinity of ZrB_2 particles while noticeably reducing their oxygen content. In contrast, H_2SO_4 and HF treatments were found to significantly change the crystallinity of ZrB_2 particles, forming impurities such as ZrO_2, which contains significant amounts of oxygen, as well as SZ. Furthermore, HF-treated ZrB_2 particles assume a rhapis shape. These results clearly demonstrate that H_2SO_4 and HF treatments do not enhance the purity of ZrB_2 particles.

The dispersibility of ZrB_2 particles were also found to be affected by acid treatment. The absolute zeta potentials of HCl- and HNO_3-treated particles exceed that of as-received commercial ZrB_2 particles. The FT-IR spectra of HCl- and HNO_3-treated particles are similar to those of the as-received ZrB_2 particles; however, their peaks corresponding to the stretching vibrations of O–H groups are more intense. Moreover, the O–H peak in the spectrum of the HCl-treated ZrB_2 particles is less intense than the corresponding peak in the spectrum of the HNO_3-treated ZrB_2 particles. These results suggest that HCl and HNO_3 treatments improve the electrostatic repulsion of ZrB_2 particles by forming hydroxyl groups on their surfaces. The as-received ZrB_2 particles show bimodal PSD while the acid-treated particles show monomodal PSD. This is because the aggregation of particles is prevented by the enhanced electrostatic repulsion between the acid-treated ZrB_2 particles. This study revealed that the oxygen content and aqueous dispersibility of ZrB_2 particles treated with HNO_3 are lower and higher, respectively, than those of ZrB_2 particles treated with HCl, H_2SO_4, and HF.

Author Contributions: Conceptualization, G.S.A.; methodology, J.C. and G.S.A.; formal analysis, J.C. and G.S.A.; resources, J.C. and G.S.A.; writing—original draft preparation, J.C. and G.S.A.; writing—review and editing, J.C. and G.S.A.; visualization, J.C. and G.S.A.; supervision, G.S.A.; project administration, G.S.A. All authors have read and agreed to the published version of the manuscript.

Funding: This research received no external funding.

Institutional Review Board Statement: Not applicable.

Informed Consent Statement: Not applicable.

Data Availability Statement: Not applicable.

Acknowledgments: This paper was supported by Korea Institute for Advancement Technology (KIAT) grant funded by the Korea Government (MOTIE) (P0017012, Human Resource Development Program for Industrial Innovation).

Conflicts of Interest: The authors declare no conflict of interest.

References

1. Levine, S.R.; Opila, J.E.; Halbig, M.C.; Kiser, J.D.; Singh, M.; Salem, J.A. Evaluation of ultra-high temperature ceramics for aeropropulsion use. *J. Eur. Ceram. Soc.* **2002**, *22*, 2757–2767. [CrossRef]
2. Wuchina, E.; Opila, E.; Opeka, M.; Fahrenholtz, W.; Talmy, I. UHTCs: Ultra-High Temperature Ceramic Materials for Extreme Environment Applications. *Electrochem. Soc.* **2007**, *16*, 30–36. [CrossRef]
3. Fahrenholtz, W.G.; Wuchina, E.J.; Lee, W.E.; Zhou, Y. *Ultra-High Temperature Ceramics: Materials for Extreme Environment Applications*; John Wiley & Sons, Inc.: Toronto, ON, Canada, 2014.
4. Telle, R.; Sigl, L.S.; Takagi, K. Boride-based hard materials. In *Handbook of Ceramic Hard Materials*; Wiley-VCH: Weinheim, Germany, 2000.

5. Guo, S.Q. Densification of ZrB_2-based composites and their mechanical and physical properties: A review. *J. Eur. Ceram. Soc.* **2019**, *29*, 995–1011. [CrossRef]
6. Jung, E.-Y.; Kim, J.-H.; Jung, S.-H.; Choi, S.-C. Synthesis of ZrB_2 powders by carbothermal and borothermal reduction. *J. Alloys Compd.* **2012**, *538*, 164–168. [CrossRef]
7. Rangaraj, L.; Divakar, C.; Jayaram, V. Fabrication and mechanisms of densification of ZrB_2-based ultra high temperature ceramics by reactive hot pressing. *J. Eur. Ceram. Soc.* **2010**, *30*, 129–138. [CrossRef]
8. Sun, C.N.; Gupta, M.C. Laser Sintering of ZrB_2. *J. Am. Ceram. Soc.* **2008**, *91*, 1729–1731. [CrossRef]
9. Shin, J.R.; Kim, B.-G.; Choi, S.-C.; Jung, Y.-G.; An, G.S. Amino Functionalization of Zirconium Diboride for High Dispersion Stability and Solid Loading. *J. Nanosci. Nanotechnol.* **2020**, *20*, 6747–6752. [CrossRef] [PubMed]
10. Zhang, S.C.; Hilmas, G.E.; Fahrenholtz, W.G. Pressureless Sintering of ZrB_2-SiC Ceramics. *J. Am. Ceram. Soc.* **2007**, *91*, 26–32. [CrossRef]
11. Wee, S.-B.; An, G.S.; Han, J.S.; Oh, H.-C.; Choi, S.-C. Co-dispersion behavior and interactions of nano-ZrB_2 and nano-SiC in a non-aqueous solvent. *Ceram. Int.* **2016**, *42*, 4658–4662. [CrossRef]
12. Pazhouhanfar, Y.; Sabahi Namini, A.; Shaddel, S.; Ahmadi, Z.; Asl, M.S. Combined role of SiC particles and SiC whiskers on the characteristics of spark plasma sintered ZrB_2 ceramics. *Ceram. Int.* **2020**, *46*, 5773–5778. [CrossRef]
13. Kashyap, S.K.; Mitra, R. Densification behavior involving creep during spark plasma sintering of ZrB_2-SiC based ultra-high temperature ceramic composites. *Ceram. Int.* **2020**, *46*, 5028–5036. [CrossRef]
14. Jung, S.-H.; Oh, H.-C.; Kim, J.-H.; Choi, S.-C.; Lee, S.-H.; Kim, H.-D. Pretreatment of zirconium diboride powder to improve densification. *J. Alloys Compd.* **2013**, *548*, 173–179. [CrossRef]
15. Han, J.S.; Lee, H.S.; Shin, J.R.; Hur, J.U.; Choi, S.-C.; Kim, H.-J.; Kim, Y.J.; An, G.S. Synthesis of nanosized zirconium diboride powder with high purity via simply purified boron carbide. *Int. J. Nanotechnol.* **2018**, *15*, 518–527. [CrossRef]
16. An, G.S.; Han, J.S.; Hur, J.U.; Choi, S.-C. Synthesis of sub-micro sized high purity zirconium diboride powder through carbothermal and borothermal reduction method. *Ceram. Int.* **2017**, *43*, 5896–5900. [CrossRef]
17. Naraparaju, R.; Maniya, K.; Murchie, A.; Fahrenholtz, W.G.; Hilmas, G.E. Effect of moisture on the oxidation behavior of ZrB_2. *J. Am. Ceram. Soc.* **2020**, *104*, 1058–1066. [CrossRef]
18. Ortiz, A.L.; Zamora, V.; Rodríguez-Rojas, F. A study of the oxidation of ZrB_2 powders during high-energy ball-milling in air. *Ceram. Int.* **2012**, *38*, 2857–2863. [CrossRef]
19. Monticelli, C.; Zucchi, F.; Pagnoni, A.; Colle, M.D. Corrosion of a zirconium diboride/silicon carbide composite in aqueous solutions. *Electrochim. Acta* **2005**, *50*, 3461–3469. [CrossRef]
20. Jung, S.H.; Choi, S.-C. Effects of particle size and oxygen contents on ZrB_2 powder for densification. *J. Korean Cryst. Growth Cryst. Technol.* **2012**, *22*, 247–253. [CrossRef]
21. Thompson, M.; Fahrenholtz, W.G.; Hilmas, G. Effect of Starting Particle Size and Oxygen Content on Densification of ZrB_2. *J. Am. Ceram. Soc.* **2011**, *94*, 429–435. [CrossRef]
22. Boch, P.; Niepce, J.-C. *Ceramic Materials Processes, Properties and Applications*; ISTE Ltd.: Arlington, VA, USA, 2007.
23. Monticelli, A.B.C.; Colle, M.D. Electrochemical Behavior of ZrB_2 in Aqueous Solutions. *J. Electrochem. Soc.* **2004**, *151*, 331–339. [CrossRef]
24. Giagloglou, K.; Payne, J.L.; Crouch, C.; Gover, R.K.B.; Connor, P.A.; Irvine, J.T.S. Zirconium Trisulfide as a Promising Cathode Material for Li Primary Thermal Batteries. *J. Electrochem. Soc.* **2016**, *163*, A3126–A3130. [CrossRef]
25. Kumar, A.; Badoni, R.P.; Singhal, S.; Agarwal, S.; Tripathi, A.R. Synthesis and characterization of zirconia-based catalyst for the isomerization of n-hexane. *Chem. Eng. Commun.* **2017**, *205*, 92–101. [CrossRef]
26. Kalinnikov, G.V.; Vinokurov, A.A.; Kravchenko, S.E.; Dremova, N.N.; Nadkhina, S.E.; Shilkin, S.P. Oxidation Behavior of Zirconium Diboride Nanoparticles. *Inorg. Mater.* **2018**, *54*, 550–557. [CrossRef]